Electrical Impedance Tomography for Assessing Ventilation/Perfusion Mismatch for Pulmonary Embolism Detection without Interruptions in Respiration

Doan Trang Nguyen[1] (*IEEE Student Member*), Aravinda Thiagalingam[2], Abhishek Bhaskaran[2], Michael A Barry[2], Jim Pouliopoulos[2], Craig Jin[1] and Alistair L McEwan[1]

***Abstract*— Recent studies have shown high correlation between pulmonary perfusion mapping with impedance contrast enhanced Electrical Impedance Tomography (EIT) and standard perfusion imaging methods such as Computed Tomography (CT) and Single Photon Emission Computerized Tomography (SPECT). EIT has many advantages over standard imaging methods as it is highly portable and non-invasive. Contrast enhanced EIT uses hypertonic saline bolus instead of nephrotoxic contrast medium that are utilized by CT and nuclear Ventilation/Perfusion (V/Q) scans. However, current implementation of contrast enhanced EIT requires induction of an apnea period for perfusion measurement, rendering it disadvantageous compared with current gold standard imaging modalities. In the present paper, we propose the use of a wavelet denoising algorithm to separate perfusion signal from ventilation signal such that no interruption in patient's ventilation would be required. Furthermore, right lung to left lung perfusion ratio and ventilation ratio are proposed to assess the mismatch between ventilation and perfusion for detection of Pulmonary Embolism (PE). The proposed methodology was validated on an ovine model (n=3, 83.7 ± 7.7 kg) with artificially induced PE in the right lung. The results showed a difference in right lung to left lung perfusion ratio between baseline and diseased states in all cases with all paired t-tests between baseline and PE yielding $p < 0.01$, while the right lung to left lung ventilation ratio remained unchanged in two out of three experiments. Statistics were pooled from multiple repetitions of measurements per experiment.**

I. INTRODUCTION

Diagnosis of Pulmonary Embolism (PE) in current practice relies heavily on imaging evidence provided by CT Pulmonary Angiogram (CTPA). However, CTPA is also sensitive to small subsegmental isolated emboli, for which anticoagulant treatment could do more harm than good [1]. Over-diagnosis and over-treatment of PE with CTPA puts unnecessary financial burden on the healthcare system as well as avoidable psychological stress on the patients and their families. At the same time, PE is also underdiagnosed as in 25% of PE patients, the initial clinical presentation is death [2]. Thus, to reduce the mortality due to PE, we propose that there is a need to detect more clinically relevant PEs in patients unsuitable for conventional imaging such as those with contrast allergy and renal failure, highly instrumented patients or pregnant women.

Electrical Impedance Tomography (EIT) is a promising medical imaging modality, which typically uses a single ring of surface external electrodes to image conductivity changes within the body. With recent successes in continuous bedside monitoring of ventilation with EIT, several groups have studied EIT using high concentration saline bolus as contrast agents [3], [4] for perfusion imaging. The results of these studies showed high correlation between EIT and standard imaging methods such as electron beam CT and SPECT. However, these studies are limited by the need for long periods of apnoea (2 minutes), highly hypertonic 20% saline contrast agent and invasive central venous access.

In the present paper, we seek to improve the clinical applicability of contrast enhanced EIT for perfusion detection by removing the need to induce an apnoea in patients for perfusion measurement. Instead, a wavelet denoising algorithm is utilised to filter out the respiration signal from the perfusion signal. The algorithm was tested on an ovine model (n=3, 83.7 ± 7.7 kg) with artificially induced PE.

II. METHOD

A. Animal Preparations

The study was conducted using methods approved by the Westmead Hospital Ethics committee for animal experiments (protocol number 5114.06.13). Three adult male sheep were pre-medicated with intramuscular xylazine (0.5 mg/kg). Anesthesia was induced with intravenous propofol (2 mg/kg) and maintained with inhaling isoflourane (2-2.5% in O2). The animals were intubated and mechanically ventilated to maintain end tidal pCO2 at 30 to 35 mmHg. Inspiratory to expiratory ratio was maintained at 1:1.5. Ventilation rate was between 10 to 14 breaths per minute. The left femoral artery was cannulated for invasive arterial blood pressure monitoring.

An Agilis catheter (8.5 Fr, St Jude Medical, USA) was introduced from the right femoral vein to provide direct contrast injection path to the right atrium via the Inferior Vena Cava. A balloon catheter (6 to 9 mm) was introduced from the right jugular vein to the right pulmonary artery tree for artificial induction of a pulmonary embolism (PE) event, following [3]. Each pulmonary occlusion and pulmonary reperfusion procedure was confirmed fluoroscopically by

Correspondence: d.nguyen@sydney.edu.au

*This work was supported by an International Postgraduate Research Scholarship from the Australian Government, an Australian Research Council grant (ARC DP110100186), The University of Sydney and Westmead Hospital.

[1]D T Nguyen, C Jin and A McEwan are with School of Electrical and Information Engineering, The University of Sydney, NSW 2006, Australia.

[2]A Thiagalingam, A Bhaskaran, M A Barry and J Pouliopoulos are with Department of Cardiology, Westmead Hospital, NSW 2150, Australia.

978-1-4244-7929-0/14/$26.00 ©2014 IEEE

injection of radiolucent contrast at the site of occlusion. Furthermore, the choice of which segment of the pulmonary artery to be occluded is such that the induced PE would be of segmental or lower level (Fig 1).

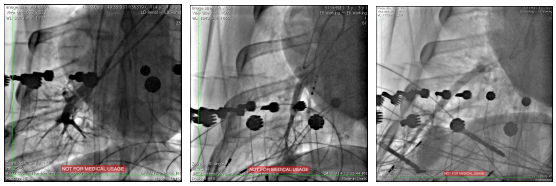

Fig. 1. Artificial pulmonary thrombolization with balloon catheters in subjects S1–3 (from left to right) . The fluoroscopic image showed the blockage of a small segment of the pulmonary artery, radiolucent contrast was injected at the tip of the balloon. When the balloon was inflated to fully block the artery, radiolucent contrast highlighted the bifurcation after the blockage, corresponding to the affected area of the induced PE. The black multipoint object seen on fluoroscopy were images of the multi-point electrodes with diameter d = 10 mm.

The skin was cleaned and shaved between the fifth and sixth intercostal space for EIT electrode ring. Following [5], multi–point bronze-coated electrodes [6] were arranged equidistantly around the animal's thorax in an approximately axial plane at the sixth intercostal space, as determined by fluoroscopy (Siemens Artis Zee, Siemens, Germany).

B. Experimental procedure

Data were acquired with three repetitions for each animal in two states: PE (balloon inflated) and baseline (balloon deflated). In each measurement, a 60 ml bolus of hypertonic saline 3% was injected into the IVC through the Agilis catheter. Injection time in each case was between 5 and 7 seconds. EIT images were acquired starting 60 seconds before the injection and ending 180 seconds after the injection, totalling 4 minutes for each measurement.

C. EIT image acquisition and reconstruction

EIT images were acquired with the 32-channel Swisstom Pioneer system (Swisstom AG, Landquart, Switzerland) with excitation frequency of 100 kHz, current amplitude 5 mA and image rate of 10 fps, utilizing a skipped-by-4 current injection and voltage measurement protocol. Standard time–difference EIT was employed. The reference voltage measurement set was the computed mean of the first one minute of recording in each case, during which time the animal was mechanically ventilated. The GREIT reconstruction algorithm [7] was utilised to reconstruct images based on an extruded sheep thorax FEM mesh, resulting in a 64×64 image for each frame. EIDORS [8] and Matlab (Mathworks, MA, USA) were utilised for all image reconstruction and processing of EIT images.

D. Analysis of EIT images

1) Wavelet filtering for perfusion estimation: A wavelet denoising algorithm implemented through thresholding of coefficients [9], [10] was employed to separate the ventilation signal and the dilution of the contrast bolus signal. The mother wavelet utilised was a Daubechies wavelet of level 4, decomposition to 8 levels [11]. Thresholdings were designed to remove all the lower levels coefficients, i.e high frequency signals, and retaining only coefficients at levels 7 and 8, i.e low frequency signals (Fig 2).

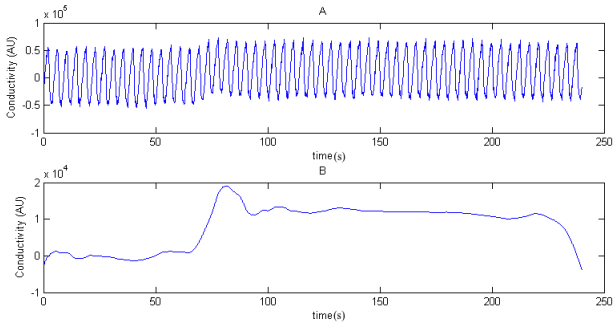

Fig. 2. Conductivity signal at a lung pixel before (A) and after wavelet denoising (B).

Following filtering, the *relative* blood volume (Q_n) reaching the two lungs based on dilution of the contrast bolus for each pixel n was computed as the area under the curve of the conductivity dilution curve at that pixel $\sigma'_n(t)$ [12], [13]:

$$Q_n = \int_{T-\epsilon_1}^{T+\epsilon_2} \sigma'_n(t)dt \tag{1}$$

where T was the time t at which the dilution $\sigma'(t)$ reached its maximum and ϵ_1 was set at 5 seconds while ϵ_2 was set at 10 seconds.

2) Identification of relevant region of interest: First the Fourier Transform of the unfiltered time conductivity signal ($\sigma_n(t)$) of each pixel n was computed. Consequently, to represent respiration (V_n), we computed the mean amplitude of all frequency bins in each pixel (n) that were within the respiration range (8 to 18 breaths per minute) [14].Two general regions of interests (ROIs), for the left lung (ROIL) and the right lung (ROIR), were defined simply as:

- ROIL contains all pixels on the *right* half of the image (pixels with horizontal position y such that $32 \leq y \leq 64$)
- ROIR contains all pixels on the *left* half of the image (pixels with $1 \leq y \leq 33$)

Then, to correctly identify each respective ROI, we opted to use a simpler method of thresholding with a low threshold (10% maximum amplitude of each respective ROI) since the accurate anatomy was not critical (as shown in Fig. 3). This step defines the actual ROIL and ROIR that would be used in later steps:

3) Ventilation and Perfusion ratio of the left and right lung: Mean blood volume distribution in each ROI was computed as:

$$\boldsymbol{Q}_{ROI} = 1/N \sum_{n=1}^{N} Q_n \tag{2}$$

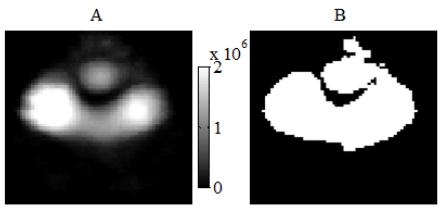

Fig. 3. (**A**): Ventilation image computed with Fourier Transform of time signal of each pixel. (**B**): Ventilation mask generated by thresholding each pixel in **A** at 10% maximum amplitude in each ROI. Patient's right is on the left of the image.

where N is the number of pixels in each ROI. In order to represent the re–distribution of perfusion due to a unilateral PE-like event, a right lung to left lung perfusion ratio (Q_{R2L}) was computed as:

$$Q_{R2L} = \boldsymbol{Q}_{ROIR}/\boldsymbol{Q}_{ROIL} \tag{3}$$

Finally, a similar ratio of left lung to right lung ventilation (V_{R2L}) was computed based on the Fourier transform of the time conductivity curve, with respiration amplitude of each ROI computed as the mean respiration amplitude of each pixel within the ROI:

$$V_{R2L} = \boldsymbol{V}_{ROIR}/\boldsymbol{V}_{ROIL} = \frac{1/N_{ROIR}\sum_{n=1}^{N_{ROIR}} V_n}{1/N_{ROIL}\sum_{n=1}^{N_{ROIL}} V_n} \tag{4}$$

III. RESULTS

A summary of the results are presented in Fig 4 with statistic drawing from the repetitive measurements in each animal experiment. In each case, we performed two-tail t-tests on the same parameter (V_{R2L} or Q_{R2L}) with and without PE induction. The null hypothesis for each pair is that there is no changes to the parameter between baseline and PE (right lung defect) state. Null hypotheses are rejected if $p < 0.01$ (99% confidence).

As shown in Fig. 4, in all cases, there were statistically significant decreases (all paired t-test gave $p < 0.01$) in the right lung to left lung perfusion ratio (Q_{R2L}) in the PE states compared with baseline:

- in S1, Q_{R2L} decreased from 1.06 ± 0.05 in baseline to 0.91 ± 0.01 in PE state;
- in S2, Q_{R2L} decreased from 0.92 ± 0.01 in baseline to 0.89 ± 0.004 in PE state;
- in S3, Q_{R2L} decreased from 0.92 ± 0.02 in baseline to 0.75 ± 0.03 in PE state.

The ventilation parameter V_{R2L} showed insignificant change between baseline and PE states in S2 and S3 ($p = 0.4$ and $p = 0.8$, respectively). However, in S1, the V_{R2L} decreased from 1.0 ± 0.04 to 0.86 ± 0.01 ($p < 0.01$).

Fig. 5 shows the perfusion map calculated with the above method at the peak of the dilution curve. The perfusion distribution in the two lung confirmed the dramatic change in Q_{R2L} between diseased (PE state) and baseline.

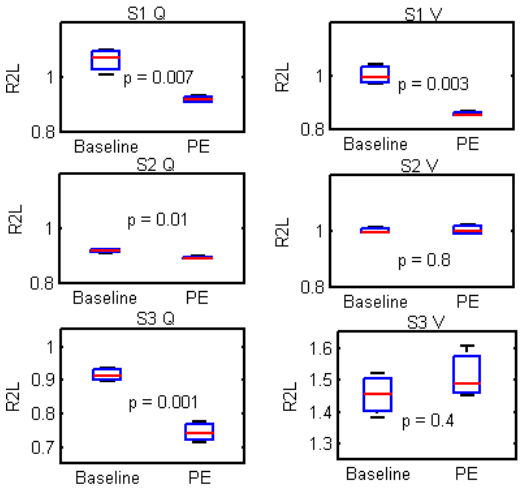

Fig. 4. Perfusion Q_{R2L} and ventilation V_{R2L} at baseline and PE in three experiments (S1–3).

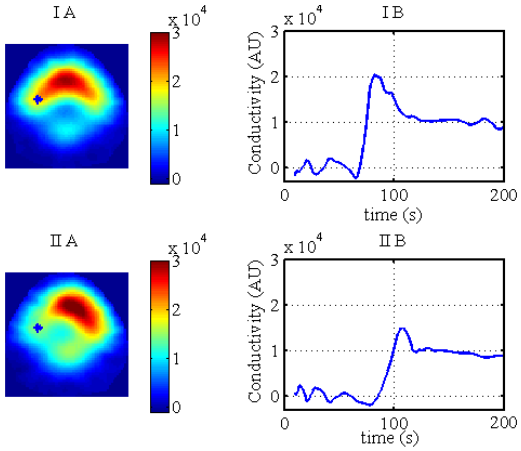

Fig. 5. Above: Perfusion image based on contrast dilution as measured with EIT after wavelet filtering of S3 at basline state (I A) and time dilution curve of a pixel (*) in the right lung (I B). Below: Perfusion image (II A) based on contrast dilution of hypertonic saline bolus as measured with EIT at PE state (part of the right lung) and time dilution curve of pixel (*) in the right lung (II B). Patient's right is on the left of the image.

IV. DISCUSSION

In this paper, we present a new paradigm for performing pulmonary perfusion scan with contrast enhanced EIT without interruption in respiration. The presented method relies on performing a wavelet denoising on the raw EIT signal to separate the contrast dilution curve from concurrent respiration signal. The decision to use wavelet filtering in place of traditional frequency filtering was because in non-mechanically-ventilated patients with pulmonary problems, breathing rate varies widely and unexpectedly. Furthermore, the time dilution signal in each pixel of the left or right lung was inherently time variant. Thus, traditional frequency filters such as FIR or IIR filters are ill-suited for filtering purposes of this signal while filtering methods based on wavelet transforms were more suitable. The method yielded contrast dilution curves that are similar in morphology to previously published studies [3], [4], which showed the contrast dilution

curve with saline had a rapid rise following injection, a fast initial wash-out phase and finally a slow washed-out phase for highly perfused pixels as shown in Fig. 2 and Fig. 5. However, the magnitude of curve reported in this paper is different from previously reported 10% change at the peak of dilution curve [3], [4], because EIT images were reconstructed for conductivity instead of impedance. As the contrast agent used in these experiments, hypertonic saline, is highly conductive, we opted for conductivity reconstruction instead of impedance, following comments in [15].

Ventilation and perfusion at each pixel were calculated based on local conductivity change acquired with EIT imaging. Ventilation was computed as the summation of amplitudes of frequencies within the respiration range [16] while perfusion of each pixel were computed as the area under the curve of the contrast dilution curve within an interval around the peak of the dilution curve from $[T - \epsilon_1]$ to $[T + \epsilon_2]$. ϵ_1 was set at 5 seconds prior to the peak of the dilution curve to avoid interference due to spreading effect of the quick rise in conductivity within the heart immediately following the injection of the contrast bolus to neighbouring pixels. ϵ_2 was set at 10 seconds after the peak of the dilution curve to capture the fast initial washout out phase of the dilution curve but not the subsequent contrast re-flow phase.

End-point assessment of the proposed algorithm on an ovine model with artificially induced PE was also presented. Two parameters, V_{R2L} and Q_{R2L} are utilised to assess the ventilation/perfusion (V/Q) mismatch between the two lungs. When an artificial embolus was induced in the right lung of each animal, the perfusion Q_{R2L} ratio decreased compared with baseline (Fig. 4, $p < 0.01$), resulted from the overall reduction of perfusion in the right lung due to the pulmonary arterial blockage. The amount of reduction in the Q_{R2L} parameter in PE states compared with baseline varied in each experiment. Factors affecting the degree of reduction in lung perfusion due to PE as measured by EIT would not only be dependent on the size of the perfusion defect caused by the embolus but also be dependent on the placement of the EIT electrode ring in reference to the affected area.

The ventilation ratios between the two lungs were not expected to change, as demonstrated in the case of S2 and S3 but not in S1. In S1, the ventilation rate were changed from 12 breaths per minute in PE states to 14 breaths per minute in baseline, while the ventilation remained the same in the other two experiments. However, it is uncertain whether the change in ventilation rate can be entirely accounted for changes in ventilation dynamics between the two lungs in the case of S1, which should be further investigated in future experiments.

V. CONCLUSION

Contrast enhanced EIT can provide the much needed alternative imaging modality to detect more clinically relevant PEs in patients unsuitable for conventional imaging such as those with contrast allergy and renal failure, highly instrumented patients or pregnant women. We showed in this paper that the combination of advanced signal processing methods including wavelet filtering, automatic ROI selection based on respiration signal and additional information on the ventilation can be used to assess ventilation/perfusion mismatch in patients. The presented work is a proof of concept, with a larger sample required to fully assess the sensitivity and specificity of the proposed paradigm.

REFERENCES

[1] R. S. Wiener, L. M. Schwartz, and S. Woloshin, "When a test is too good: how ct pulmonary angiograms find pulmonary emboli that do not need to be found," *BMJ*, vol. 347, no. f3368, 2013.

[2] A. S. Go, D. Mozaffarian, V. L. Roger, E. J. Benjamin, J. D. Berry, W. B. Borden, D. M. Bravata, S. Dai, E. S. Ford, C. S. Fox, S. Franco, H. J. Fullerton, C. Gillespie, S. M. Hailpern, J. A. Heit, V. J. Howard, M. D. Huffman, B. M. Kissela, S. J. Kittner, D. T. Lackland, J. H. Lichtman, L. D. Lisabeth, D. Magid, G. M. Marcus, A. Marelli, D. B. Matchar, D. K. McGuire, E. R. Mohler, C. S. Moy, M. E. Mussolino, G. Nichol, N. P. Paynter, P. J. Schreiner, P. D. Sorlie, J. Stein, T. N. Turan, S. S. Virani, N. D. Wong, D. Woo, and M. B. Turner, "Heart disease and stroke statistics–2013 update: A report from the american heart association," *Circulation*, vol. 127, pp. e6–e245, 2013.

[3] I. Frerichs, J. Hinz, P. Herrmann, G. Weisser, G. Hahn, M. Quintel, and G. Hellige, "Regional lung perfusion as determined by electrical impedance tomography in comparison with electron beam CT imaging.," *IEEE transactions on medical imaging*, vol. 21, pp. 646–52, June 2002.

[4] J. B. Borges, F. Suarez-Sipmann, S. H. Bohm, G. Tusman, A. Melo, E. Maripuu, M. Sandström, M. Park, E. L. V. Costa, G. Hedenstierna, and M. Amato, "Regional lung perfusion estimated by electrical impedance tomography in a piglet model of lung collapse," *Journal of Applied Physiology*, vol. 112, pp. 225–236, Sept. 2011.

[5] D. T. Nguyen, R. Kosobrodov, M. A. Barry, W. Chik, C. Jin, T. I. Oh, A. Thiagalingam, and A. McEwan, "Electrode-Skin contact impedance: In vivo measurements on an ovine model," *Journal of Physics: Conference Series*, vol. 434, 2013. Conference Proceedings of the XV Int. Conf. on Electrical Bio-Impedance and XIV Conf. on Electrical Impedance Tomography.

[6] R. Cardu, P. Leong, C. Jin, and A. McEwan, "Electrode contact impedance sensitivity to variations in geometry," *Physiological measurement*, vol. 33, pp. 817–830, May 2012.

[7] A. Adler, J. H. Arnold, R. Bayford, A. Borsic, B. H. Brown, P. Dixon, T. J. Faes, I. Frerichs, H. Gagnon, Y. Gärber, B. Grychtol, G. Hahn, W. R. B. Lionheart, A. Malik, R. P. Patterson, J. Stocks, A. Tizzard, N. Weiler, and G. K. Wolf, "Greit: A unified approach to 2d linear eit reconstruction of lung images," *Physiological measurement*, vol. 30, pp. S35–S55, June 2009.

[8] A. Adler and W. R. B. Lionheart, "Uses and abuses of eidors: An extensible software base for eit," *Physiological measurement*, vol. 27, pp. S25–S42, May 2006.

[9] M. Lavielle, "Detection of multiple changes in a sequence of dependent variables," *Stochastic Processes and their Applications*, vol. 83, p. 79102, 1999.

[10] D. Donoho and I. Johnstone, "Ideal spatial adaptation by wavelet shrinkage," *Biometrika*, vol. 81, no. 3, p. 425455, 1994.

[11] I. Daubechies, "Ten lectures on wavelets," *CBMS-NSF conference series in applied mathematics, SIAM Ed.*, 1992.

[12] H. Uematsu, D. L. Levin, and H. Hatabu, "Quantification of pulmonary perfusion with mr imaging: recent advances," *European Journal of Radiology*, vol. 37, pp. 155–163, Mar. 2001.

[13] Y. Lin, S. Tsai, T. Huang, H. Chung, Y. Huang, F. Wu, C. Lin, N. Peng, and M. Wu, "Inflow-weighted pulmonary perfusion: comparison between dynamic contrast-enhanced mri versus perfusion scintigraphy in complex pulmonary circulation," *Journal of Cardiovascular Magnetic Resonance*, vol. 15, no. 21, 2013.

[14] D. Ferrario, B. Grychtol, A. Adler, J. Solà, S. H. Böhm, and M. Bodenstein, "Toward morphological thoracic EIT: major signal sources correspond to respective organ locations in CT," *IEEE Transactions on Biomedical Engineering*, vol. 59, pp. 3000–8, Nov. 2012.

[15] N. C. Hellige, G. Hahn, and G. Hellige, "Comment on Borges et al. Regional lung perfusion estimated by electrical impedance tomography in a piglet model of lung collapse," *Journal of Applied Physiology*, vol. 112, p. 2127, 2012. Letter to the Editor.

[16] M. Bodenstein, M. David, and K. Markstaller, "Principles of electrical impedance tomography and its clinical application.," *Critical care medicine*, vol. 37, pp. 713–24, Feb. 2009.